Appl. Phys. A
DOI 10.1007/s00339-014-8897-y

Applied Physics A
Materials Science & Processing

RAPID COMMUNICATION

Femtosecond laser melting and resolidifying of high-temperature powder materials

Bai Nie · Huan Huang · Shuang Bai · Jian Liu

Received: 18 September 2014 / Accepted: 11 November 2014
© Springer-Verlag Berlin Heidelberg 2014

Abstract Though the development of laser additive manufacturing has achieved great success and has been widely used for various materials, it still has limited applications for materials with high melting temperature. In this report, we explore the feasibility of using femtosecond lasers to melt and resolidify these materials, as femtosecond lasers can generate MW-level peak power and create high local temperature. Tungsten, which has the highest melting point (3,422 °C) among all the elements, and several other materials with melting temperature higher than 3,000 °C are chosen for the proof of concept. For the first time, femtosecond laser melting and resolidification of these high-temperature powder materials is achieved. Fabricated samples are characterized by scanning electron microscope and energy-dispersive X-ray spectroscopy. The results manifest that femtosecond laser melting can be an ideal solution for laser additive manufacturing of high-temperature materials.

1 Introduction

Laser additive manufacturing (AM) has greatly been developed since it was introduced in late 1980s and early 1990s [1], especially with the boom of three-dimensional (3D) printing. It has been proved to be an efficient, robust, and cost-effective way for the next generation manufacturing. Selective laser melting (SLM) is one of the most important among many laser manufacturing methods [2, 3]. By selectively melting the source materials (usually powders), free-form products with complex structures can be fabricated. Their mechanical properties are comparable to or even better than their normal bulk parts. Laser melting of materials such as Fe, Ni, and Cu has been widely demonstrated with continuous-wave (CW) or long-pulse lasers [3, 4]. These materials all have melting points lower than 2,000 °C. However, laser AM of high-temperature materials (above 3,000 °C), such as refractory metals and ceramics, still remains challenging with current SLM processes. Only partial melting of tungsten powders was achieved using CW lasers (usually 100 W power level), where the particles just melt superficially and form interconnections between them [5]. Therefore, the fabricated parts do not reach substantial densification, which is detrimental to most applications.

Compared with CW or long-pulse lasers, fs lasers can deliver several orders of magnitude higher peak power, more than MW. Due to the significantly high peak power and ultrashort pulse duration, fs lasers have fundamental differences in laser–material interactions, in contrast to CW or long-pulse lasers [6, 7]. It has been simulated that materials irradiated with a high-repetition fs laser can reach temperature above 6,000 °C [8]. Though fs lasers have largely been used for various material processing such as drilling [9], micro-structuring [10], and glass welding [11], their applications in laser AM have not been extensively studied yet. Previously, fs lasers were used to melt nanometer tungsten powders in a very small scale [12]. However, micro-scale materials are commonly used in practical laser AM. They have very different thermal properties compared with those in nanoscale and are much harder to melt. It is known that the threshold laser fluence for metal melting is proportional to its particle size [13, 14] or thickness [15], due to the change of effective thermal conductivity. In order to fully investigate the possibility of

B. Nie (✉) · H. Huang · S. Bai · J. Liu
Polaronyx, Inc., 2526 Qume Drive, Suites 17 & 18, San Jose, CA 95131, USA
e-mail: bnie@polaronyx.com

Published online: 26 November 2014

fs laser AM of high-temperature materials, laser melting micrometer-sized particles needs to be investigated.

Here, we demonstrated the full melting of micrometer-sized high-temperature powder materials using a fs fiber laser and explored the possibility of utilizing fs laser for additive manufacturing. Several materials with very high melting temperature, such as tungsten, rhenium, and ceramics, were selected for evaluation. A few processing parameters were varied to study the dependence of the powder melting. Millimeter-scale-reformed parts from entirely melted powders were achieved. To our best knowledge, it is the first time that a fs laser is employed to melt and resolidify high-temperature powder materials. Scanning electron microscope (SEM, FEI NanoSEM630) and energy-dispersive X-ray spectroscopy (EDX, Oxford Aztec) measurements were taken at the cross-sections of the fabricated samples.

2 Experimental setup

A 50-W Yb fiber laser (mJ Uranus, PolarOnyx Laser, Inc., California), with central wavelength of 1,030 nm, was used in the experiments. The laser was operated at 1 MHz and delivered pulse energy up to 50 µJ. Output pulses were compressed to have a full-width-half-maximum (FWHM) pulse duration of 400 fs. The corresponding peak power is 125 MW. As shown in Fig. 1, the laser beam passed through

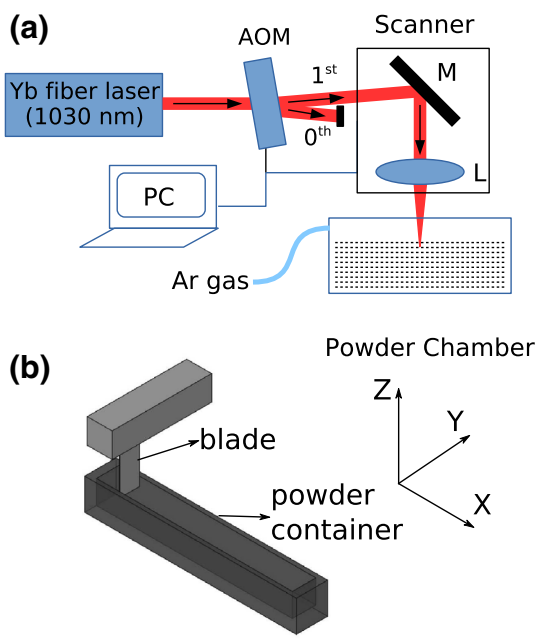

Fig. 1 **a** Schematic of the experimental setup. *AOM* acoustic optical modulator, *M* galvanic mirrors, *L* lens. **b** Sketch of powder preparation setup.The powder container is made of aluminum and the transparency is just made for the better visibility

an acoustic optical modulator (AOM, Gooch & Housego, Florida). The first-order diffraction of the AOM was picked up and guided through a galvanic-mirror-enabled scanner. The zeroth-order diffraction of the AOM was blocked or used for monitoring the laser power. The laser beam going through the scanner was focused by a lens with 82-mm-long focal length and had a FWHM diameter of 20 µm on target. The focused laser beam was raster-scanned on the powder surface. The maximum laser average power measured after the scanner was 39 W. Considering the loss through the fused silica window of the powder chamber, the maximum average power reached on powder surface was about 35 W, resulting in a pulse energy of 35 µJ. A few parameters, such as pulse energy and scanning speed, were varied to study their impact on the powder melting. Laser on/off and pulse energy variation were controlled by the AOM, which was synchronized with the scanner.

The powders were deposited in an aluminum container (50 mm × 6 mm × 6 mm) and not compressed. A blade mounted on a translation stage was used to make an even powder surface and control the thickness of the powder bed. The powder bed had a surface area of 50 mm × 6 mm and a thickness around 3 mm. The powder container was placed in a processing chamber filled with industrial standard argon (Ar) gas to prevent the oxidation. During experiments, only one layer (20 mm × 1 mm size) of powders was exposed to the laser. The area was scanned line by line with a pitch distance of 20 µm. Each line was 20 mm long and scanned along the x direction (Fig. 1b). Then, the laser beam shifted along y direction (Fig. 1b) by the pitch distance and scanned the next line. The powder bed was not melted up to the bottom of the powder container. Tungsten was chosen as the main material for investigation, since it has the highest melting temperature (3,422 °C) among all the elements. Its heat conductivity at room temperature is 137 $W(mK)^{-1}$, a couple of times higher than other high-temperature materials. The combination of high melting point and high conductivity makes it extremely difficult to achieve full melting by conventional SLM processes. The tungsten powders (Atlantic Equipment Engineers, New Jersey) used here have an average size of 4.7 µm in diameter (Fig. 2b), and the single powder shape is polyhedral (Fig. 2a). In Fig. 2c, the histogram of size distribution, analyzed by ImageJ, shows that most of the particles are within 1–10 µm. The purity of the powder is 99.9 % as specified by the vendor and confirmed by the EDX measurement. The SLM-processed tungsten parts were examined and characterized in term of micro-structure and element analysis. The cross-sections of the samples were prepared and polished for SEM image. EDX was also conducted on the cross-sections to analyze the element concentrations.

3 Experimental results

A few parameters such as pulse energies and scan speeds were studied in our experiment. Pulse repetition rate was fixed at 1 MHz that was optimal for our processes as suggested by the previous work [8] and our experiences. The sample shown in Fig. 3 was fabricated with an average laser power of 35 W on target, corresponding to a pulse energy of 35 µJ at 1 MHz repetition rate. With a scanning speed of 7.5 mm/s, the tungsten powders were continuously melted. The laser beam was irradiated from the upside of the sample as shown in Fig. 3a. The melted and resolidified tungsten layer was in between 25 and 50 µm. The non-uniform thickness of the melted layer was due to the lack of solid substrate and loose powder bed. As shown in Fig. 3b, uniform cross-section was observed for the fully melted region, which obviously differentiates from the non-melted powders. No porous structure or feature with the size of original particles (Fig. 2) was observed on the cross-section and this indicated the full melting of the tungsten powders.

Element analysis of the melted region was conducted by EDX (Fig. 3c). By eliminating the extra elements (carbon from the mounting media) introduced from the SEM sample preparation, pure composition of tungsten was detected. Though tungsten can be easily oxidized at high temperature [16], the Ar gas did successfully isolate the processed tungsten from being oxidized. This is very important for practical laser AM, since the purity of the fabricated parts can largely affect their mechanical properties and applications.

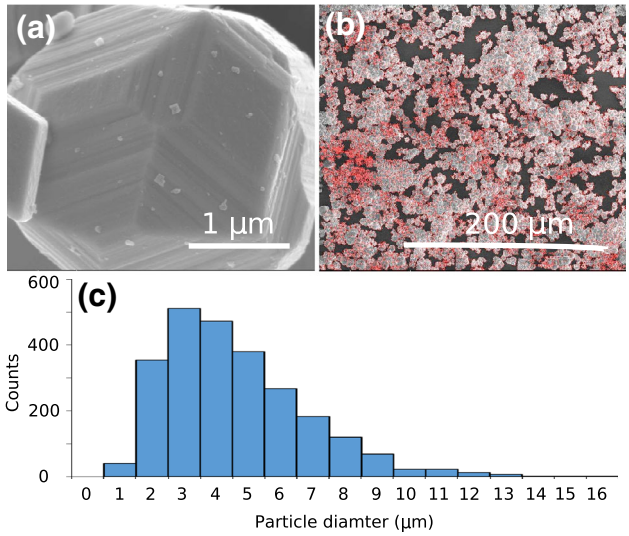

Fig. 2 **a** SEM of single tungsten particle. *Scale bar* 1 µm. **b** SEM of tungsten powders in large scale. *Red lines* fitted outlines of individual powders by ImageJ. **c** Histogram of the size distribution of tungsten powders. *Scale bar* 200 µm. *Vertical axis* number of particles for corresponding particle diameters

It was found that there were some 100-nm holes on the cross-section of the fully melted tungsten, using higher magnification SEM (Fig. 4a). Considering the fine size of the holes and that no structure of the original particle was found, it is unlikely that these holes were formed due to partial melting. We believe that it was due to the exceptionally high temperature (higher than the boiling point) generated in the molten pool. As the temperature rises above the boiling point (5,555 °C for tungsten), the boiled liquid splashes and cannot form fully densed solid [17]. Lower laser pulse energy and faster scanning speed are expected to result in lower temperature. By reducing the pulse energy to 22.5 µJ and increasing the scan speed to 20

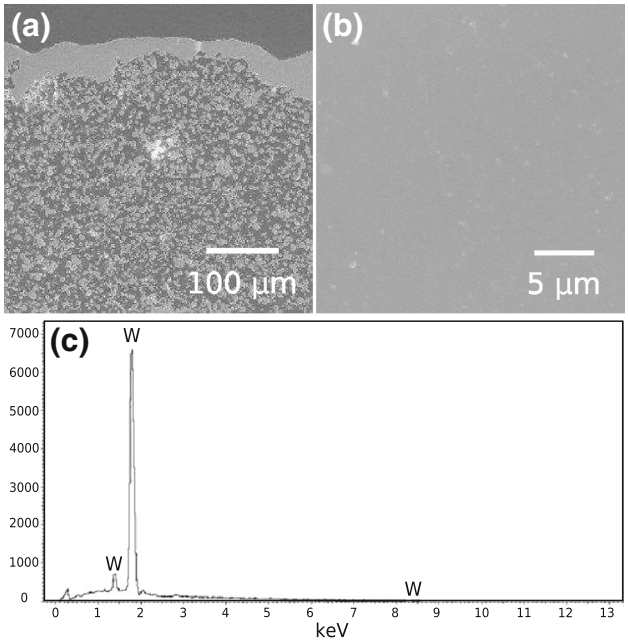

Fig. 3 **a** Cross-sectional SEM images of the fabricated sample, with fully melted tungsten and un-melted powders. *Scale bar* 100 µm. **b** High-magnification cross-sectional SEM of the fully melted region as shown in **a**. *Scale bar* 5 µm. **c** EDX result of the fully melted region (inlet)

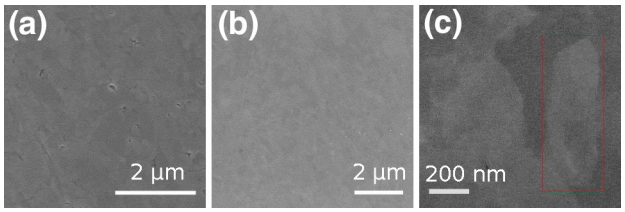

Fig. 4 **a** SEM images of the cross-section of melted tungsten with 35 µJ pulse energy and 7.5 mm/s scan speed. *Scale bar* 2 µm. **b** SEM images of the cross-section of melted tungsten with 22.5 µJ pulse energy and 20 mm/s scan speed. *Scale bar* 2 µm. **c** 1 µm × 1 µm area from **b** with ×200,000 magnification. *Red rectangle* is used to illustrate the single grain. *Scale bar* 200 nm

mm/s, more uniform cross-section of the melted sample was obtained. Checked with high-magnification SEM (Fig. 4b, c), no small hole or crack was observed. This indicates that the temperature was still high enough for full melting, but stayed below the boiling point. However, real-time in situ temperature measurement will be required to confirm this.

In both cases, reformed grains as small as a few hundred nanometers were obtained (Fig. 4). As the heating and cooling time during fs laser radiation is very fast, there is no time for the grains to grow large. The fine grain size is beneficial for the final products, since finer grains result in higher strength and toughness [18]. The mechanical property measurements will be taken as larger-scaled samples are fabricated.

Another important metal with high melting temperature, rhenium, was also used for evaluation. Rhenium has the third highest melting temperature (3,182 °C) and the highest boiling temperature (5,596 °C) among all the elements. The rhenium powders (Atlantic Equipment Engineers, New Jersey) have very different particle profiles (Fig. 5a) compared to tungsten (Fig. 2a), and their sizes are within 1–20 µm. Meanwhile, they have lower flowability and show strong agglomeration. Similar to the results of tungsten, fully melted and resolidified rhenium without (Fig 5b) and with (Fig. 5c) small holes was obtained by choosing different processing paramteres.

Additionally, high-temperature ceramics, such as hafnium diboride (melting point 3,250 °C) and zirconium diboride (melting point 3,246 °C), were also tested, as shown in Fig 6. The SEM images of the original powders (left column in Fig 6) and laser-melted samples (right column in Fig. 6) are compared. Though the laser parameters were not fully optimized, it is clearly seen that powders were fully melted and resolififyed densely. Improvement on the melting processes for these materials, such as multi-layer melting, is still ongoing. Additionally, the variation of powder shape may also affect the melting results, which will need more investigation for fs laser melting.

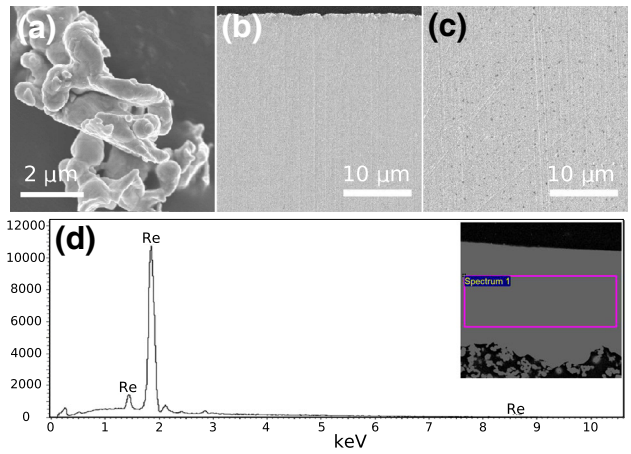

Fig. 5 Results of rhenium. **a** SEM of rhenium powder before melting. *Scale bar* 2 µm. **b** Fully melted rhenium without small holes. *Scale bar* 10 µm. **c** Fully melted rhenium with small holes. *Black dots* nanometer scale holes generaterated during the process. *Scale bar* 10 µm. **d** EDX result of the fully melted rhenium on an area of 70 µm × 23 µm. *Scale bar* 10 µm

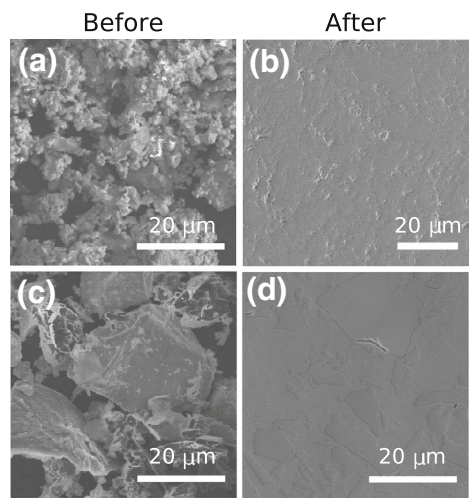

Fig. 6 *Left column* SEM of hafnium diboride (**a**) and zirconium diboride (**c**) powders before laser melting; *right column* SEM of melted hafnium diboride (**b**) and zirconium diboride (**d**). *Scale bar* 20 µm

4 Summary and outlook

For the first time, full melting of high-temperature powder materials was demonstrated with a high-energy fs fiber laser. In common, several evaluated materials all have melting temperature above 3,000 °C. The processed samples were examined and characterized by SEM and EDX. The temperature of the molten pool can be controlled by varying processing parameters, which is critical for obtaining fully densed parts. Other than exploring the feasibility of melting high-temperature materials, this demonstration also lays out a solid foundation for future 3D printing with fs lasers. We think that it can largely benefit the high-temperature products, such as engines and nozzles for aerospace and auto industry, and miniaturized biomedical devices. Furthermore, this method is not limited to high-temperature material. It can as well apply to other metals and ceramics to create unique features or functions. More thorough investigation of this process is ongoing and will be reported in the near future.

References

1. J.P. Kruth, CIRP Ann. Manuf. Technol. **40**(2), 603 (1991)
2. W.M. Steen, J. Mazumder, K.G. Watkins, *Laser Material Processing* (Springer, Berlin, 2003)
3. J.P. Kruth, L. Froyen, J. Van Vaerenbergh, P. Mercelis, M. Rombouts, B. Lauwers, J. Mater. Process. Technol. **149**(1), 616 (2004)
4. F. Abe, K. Osakada, M. Shiomi, K. Uematsu, M. Matsumoto, J. Mater. Process. Technol. **111**(1), 210 (2001)
5. D. Zhang, Q. Cai, J. Liu, Mater. Manuf. Process. **27**(12), 1267 (2012)
6. S. Anisimov, B. Kapeliovich, T. PerelMan, Zh. Eksp. Teor. Fiz **66**(776), 375 (1974)
7. B. Chichkov, C. Momma, S. Nolte, F. Von Alvensleben, A. Tünnermann, Appl. Phys. A **63**(2), 109 (1996)
8. S. Eaton, H. Zhang, P. Herman, F. Yoshino, L. Shah, J. Bovatsek, A. Arai, Opt. Express **13**(12), 4708 (2005)
9. G. Kamlage, T. Bauer, A. Ostendorf, B. Chichkov, Appl. Phys. A **77**(2), 307 (2003)
10. T.H. Her, R.J. Finlay, C. Wu, S. Deliwala, E. Mazur, Appl. Phys. Lett. **73**(12), 1673 (1998)
11. I. Miyamoto, A. Horn, J. Gottmann, D. Wortmann, F. Yoshino, Zvaranie/Svarovani **60**(3–4), 59 (2011)
12. R. Ebert, F. Ullmann, D. Hildebrandt, J. Schille, L. Hartwig, S. Kloetzer, A. Streek, H. Exner, J. Laser Micro/Nanoeng. (JLMN) **7**(1), 38 (2012)
13. J. Huang, Y. Zhang, J. Chen, J. Heat Transf. **134**(1), 012401 (2012)
14. Y. Son, T.W. Lim, J. Yeo, S.H. Ko, D.Y. Yang, in 10th IEEE Conference on Nanotechnology (IEEE-NANO), 2010 (IEEE, 2010), pp. 390–393
15. I.H. Chowdhury, X. Xu, Numer. Heat Transf. A Appl. **44**(3), 219 (2003)
16. E. Lassner, W.D. Schubert, *Tungsten: Properties, Chemistry, Technology of the Elements, Alloys, and Chemical Compounds* (Springer, Berlin, 1999)
17. M. Shiomi, A. Yoshidome, F. Abe, K. Osakada, Int. J. Mach. Tools Manuf. **39**(2), 237 (1999)
18. A.C. Reardon, Metallurgy for the Non-metallurgist (ASM International, Almere, 2011)